

# Novel composite zinc-alginate hydrogels with activated charcoal aimed for potential applications in multifunctional primary wound dressings

Andrea Osmokrovic<sup>a</sup>, Ivan Jancic<sup>b</sup>, Ivona Jankovic- Castvan<sup>a</sup>, Predrag Petrovic<sup>c</sup>, Marina Milenkovic<sup>b</sup>, Bojana Obradovic<sup>a</sup>

<sup>a</sup>Faculty of Technology and Metallurgy, University of Belgrade, Karnegijeva 4, 11000 Belgrade, Serbia

<sup>b</sup>Faculty of Pharmacy, University of Belgrade, Vojvode Stepe 450, 11000 Belgrade, Serbia

<sup>c</sup>Innovation Center of the Faculty of Technology and Metallurgy, Karnegijeva 4, 11000 Belgrade, Serbia

## Abstract

Composites based on Zn-alginate hydrogels in the form of beads were produced by extrusion of a suspension containing 0.5 % w/w of alginate and 20 % w/w of activated charcoal (AC) with the intent to simultaneously release two active agents, Zn<sup>2+</sup> and AC particles, in a physiological-like environment. The obtained composite beads were analyzed by FE-SEM and characterized regarding textural parameters, as well as Zn<sup>2+</sup> and AC release kinetics in the physiological saline solution. Zn<sup>2+</sup> ions were quickly released reaching the equilibrium concentration within the first hour in the contrary to the release of AC particles, which was described by internal diffusion with the apparent diffusion coefficient of approximately 10<sup>-13</sup> m<sup>2</sup> s<sup>-1</sup>. Potential functionality of the obtained beads was evaluated regarding antibacterial activity in suspensions of the standard bacterial strain *Escherichia coli* 25922. The observed strong bactericidal effects were related to the quick release of Zn<sup>2+</sup> that was not affected by AC. Thus, taking into account results of this study, as well as high sorption capacity of alginate hydrogel, efficiency of AC to adsorb malodor and tissue degradation products and positive effects of Zn<sup>2+</sup> on wound healing, the obtained composites have shown promising potentials for applications as multifunctional wound dressings.

**Keywords:** zinc ions; activated charcoal; alginate hydrogels; antibacterial activity; wound dressing

Available online at the Journal website: <http://www.ache.org.rs/HI/>

SCIENTIFIC PAPER

UDC 615.4:616-001:620.017

Hem. Ind. 73 (1) 37-46 (2019)

## 1. INTRODUCTION

Development of modern wound dressings aims at achieving multiple actions in wound treatment such as enhancement of healing, prevention and reduction of infections, malodour treatment and management of exudate. Historically, wound care has been focused on curing the underlying disease and healing the wound. More recently, it has been recognized that wounds and especially chronic wounds, have an enormous psychological impact on the quality of life of the patient, also (e.g. causing social isolation, withdrawal from daily activities, poor self-esteem and embarrassment) that instigates suffering for the patient's family. Out of all symptoms associated with chronic wounds, the offensive smell is often described as the symptom causing the greatest distress to patients [1-2] because it may be constantly detectable and can trigger gagging and vomiting reflexes. It is associated with the smell of rotten flesh and is caused by bacterial infection in devitalized tissue within the wound [3]. Moreover, nurses also frequently recognize malodor as one of the symptoms the most difficult to treat [1-2,4].

Another frequent problem for patients affected by chronic wounds is heavy exudate. Chronic wounds such as malignant fungating wounds can produce large amounts of exudate, sometimes over a liter per day [5]. Such high liquid quantities are extremely difficult to manage since the exudate often leaks through the dressing, soils the clothing and increases the risk of maceration of the peri-wound skin [6,7].

In order to address these very unpleasant symptoms, many modern wound dressings have several adlayers providing different functions such as absorption of the excess fluid or adsorption of malodor (e.g. Carboflex<sup>®</sup>, ConvaTec; Carbonet<sup>®</sup>, Smith&Nephew; Clinisorb<sup>®</sup>, Clinimed Ltd). The absorption layer, usually a hydrogel, is placed in direct contact with the wound tissue and its fluids. On the other hand, the adsorption layer, often made of activated carbonized cloth,

Correspondence: Andrea Osmokrovic, Faculty of Technology and Metallurgy, University of Belgrade, Karnegijeva 4, 11000 Belgrade, Serbia, Tel.: +381 11 3303 609, Fax: +381 11 3370 387

e-mail: [aosmokrovic@tmf.bg.ac.rs](mailto:aosmokrovic@tmf.bg.ac.rs)

Paper received: 29 June 2018

Paper accepted: 27 January 2019

<https://doi.org/10.2298/HEMIND180629003O>



is always placed in-between other layers without the possibility to establish direct contact with the wound products. Finally, antimicrobial activity is achieved by incorporation of an antimicrobial agent (*e.g.* iodine as in Iodozyme™, ArchiMed; silver as in Actisorb™ Silver 220, Systagenix and Acticoat™, Smith&Nephew, *etc.*).

One of the most widely used hydrogels in wound dressings is Ca-alginate due to biocompatibility, softness, flexibility and high sorption capacity. Additionally, as the hydrogel absorbs wound exudates, calcium ions are exchanged with Na<sup>+</sup> and released in the wound area acting as a haemostatic agent and reducing the coagulation time as well as stimulating keratinocyte differentiation and increasing fibroblast proliferation [8,9]. We have recently shown that dressings based on Ca-alginate induced faster healing of second degree burns in rats as compared to a colloid solution based on Na-alginate, which was attributed to additional stimuli of released Ca<sup>2+</sup> [10]. Ca-alginate fibers have been also investigated as carriers to deliver zinc, silver and other active ingredients that are beneficial to wound healing [11]. Zinc is an essential element for microorganisms and higher organisms as well, and it is involved in many vital cellular reactions at its low endogenous concentrations [12,13]. Zn<sup>2+</sup> is essentially nontoxic to higher organisms [14] because its concentration is regulated by several transporters [15,16]. On the other hand, Zn<sup>2+</sup> can be cytotoxic to prokaryotes at concentrations above ~10<sup>-4</sup> M because adsorption of Zn<sup>2+</sup> to cell membranes cannot be controlled. Therefore, at these supra-physiological concentrations, zinc ions are allowed to entry inside cells and induce cytotoxic effects [17,18]. Antimicrobial properties of Zn<sup>2+</sup> have been known since a long time, both against bacterial [19-21] and fungal strains [22]. In addition, Zn<sup>2+</sup> has a positive impact on wound healing. Specifically, it serves as a cofactor in numerous transcription factors and enzyme systems including zinc-dependent matrix metalloproteinases that augment auto-debridement and keratinocyte migration during wound repair [23,24]. Zinc calcium alginate dressings have been produced commercially (Kendall™ Zinc Calcium Alginate Dressings, Covidien, MA) with the goal to provide ion exchange during application in the wound and help initiating the healing process due to released Ca<sup>2+</sup> and Zn<sup>2+</sup>.

In this work, we aimed at devising a composite system based on Zn-alginate hydrogel that will simultaneously provide several functions in potential wound treatment. Along with exudate absorption by the hydrogel and controlled release of Zn<sup>2+</sup> to induce antimicrobial effects, as well as enhance healing, we have included activated charcoal (AC) particles in order to achieve adsorption of locally released toxins and degradation products as well as malodor. Many different studies have shown that AC can adsorb bacteria, viruses and other biochemical substances *in vitro* and *in vivo* [25-29]. In addition, AC particles can be tailored to have predominantly meso- and macroporous structure and thus, be a more suitable adsorbent than the commonly used microporous carbonized cloth and not just for removal of small volatile molecules responsible for malodor but for adsorption of bacteria and tissue degradation products as well. We have focused on incorporation of AC particles in the Zn-alginate hydrogel that will be released in a controlled manner upon the contact with physiological fluids that contain Na ions. Functionality of such a system highly depends on the release kinetics of AC particles and Zn<sup>2+</sup> from the alginate matrix as well as on their mutual interaction. Accordingly, the goal of this work was to produce and characterize zinc alginate/activated charcoal (ZnA/AC) composite hydrogels in the form of beads, to investigate release profiles of AC and Zn<sup>2+</sup> as well as to test functionality of the obtained composite regarding the antimicrobial activity.

## 2. MATERIALS AND METHODS

### 2. 1. Materials

Medium viscosity sodium alginate (A2033, molecular weight = 80.000–120.000, mannuronic (M) to guluronic (G) residue ratio M/G = 1.56) and zinc nitrate hexahydrate were purchased from Sigma (St. Louis, MO). Activated charcoal (AC) as a fine powder (MEKS 95) was purchased from Trayal (Krusevac, Serbia), NaCl from Centrohema (Stara Pazova, Serbia), while sodium citrate and tryptic soy (TS) broth were supplied from Himedia (Mumbai, India). The *Escherichia coli* strain (10536) originates from American Type Culture Collection (Rockville, MD).

### 2. 2. Preparation of composite beads

Zinc alginate/activated charcoal (ZnA/AC) beads were prepared by mixing fine AC powder and the aqueous solution of sodium alginate at the concentrations of 20 % w/w AC and 0.5 % w/w alginate using the mechanical stirrer Ultra-Turrax® T25 (Janke and Kunkel Ika-Labortechnik, Staufen, Germany) at 20000 rpm for 5 min. The obtained suspension was extruded using a syringe through a blunt edge stainless steel needle (16G) and the resulting droplets were collected in a gelling bath (1.8 % w/w Zn[NO<sub>3</sub>]<sub>2</sub>·6H<sub>2</sub>O) forming insoluble beads. The beads were left in the bath for additional 30 min to complete gelling, followed by washing in distilled water for several times. The obtained ZnA/AC beads were further air – dried at room temperature until the constant weight. Control zinc alginate (ZnA) beads were prepared in the same manner by using the aqueous 0.5 % w/w Na-alginate solution.

### 2. 3. Release kinetics

AC release kinetics from ZnA/AC beads was studied in physiological saline solution (0.9 % w/w NaCl) over a 5-day period. Dry beads [corresponding to 2 g wet weight] were added to 20 ml of the solution in closed 100 ml Erlenmeyer flasks placed in a shaking water bath at  $37 \pm 0.1$  °C at 120 rpm. At predetermined time intervals, liquid samples (0.1 ml) were collected for UV-Vis analysis while the same volume of the fresh physiological saline solution was added to each flask. All experiments were carried out in triplicates.

The capacity of ZnA and ZnA/AC beads to release  $Zn^{2+}$  was investigated under the described conditions in triplicates. At different time points, 0.3 ml samples were collected and replaced with fresh saline solution. Samples were then centrifuged at 5000 g for 5 min in order to remove AC particles from the solutions and  $Zn^{2+}$  concentrations were determined by flame atomic absorption spectrometry.

### 2. 4. Antibacterial activity

Antibacterial activity was investigated in a suspension of one standard strain, Gram negative *Escherichia coli* ATCC 25922. Active cultures were prepared by transferring a loopful of cells from the stock into tubes that contained 10 ml of physiological saline solution (0.9 % w/w NaCl). Suspensions were adjusted to 0.5 McFarland standard turbidity (corresponding to  $1.5 \times 10^8$  colony forming units (CFU/ml)). The bacterial cultures were further diluted with physiological saline solution to the final concentration of  $10^7$  CFU/ml.

Dry ZnA and ZnA/AC beads (corresponding to 4 g wet weight) were added to 100 ml Erlenmeyer flasks followed by addition of 10 ml of sterile TS broth. Aliquots of 0.1 ml bacterial suspension were inoculated in each flask so that the initial number in TS broth was approximately  $10^5$  CFU/ml. The prepared samples were incubated at 37 °C for 24 h. Bacterial cultures in TS broth without the beads served as a positive control and TC broth alone as a negative control. Also, cultures with AC powder (1.2 g corresponding to the AC amount in ZnA/AC beads added to flasks) served as an additional control. At two incubation time points (1 and 24 h), 1 ml liquid samples were withdrawn aseptically from each flask and centrifuged (Centrifuge 5804, Eppendorf, Canada) at 600 g for 10 min in order to remove AC particles. Then, 0.1 ml of the supernatant was withdrawn and cultured on TS agar in a Petri dish. Agar plates were incubated at 37 °C for 24 h and numbers of bacterial colonies were assessed to obtain the number of viable cells in suspension.

### 2. 5. Analytical methods

#### 2. 5. 1. UV-Vis spectroscopy

UV-Vis spectroscopy (UV-3100 spectrophotometer, MAPADA Instruments, Shanghai, China) was used to examine the presence of AC in saline solutions. UV-Vis spectroscopy of AC suspensions in the wavelength range from 200 to 1000 nm did not show any absorption peak so the wavelength of 600 nm was chosen to directly apply the Beer-Lambert law [30]. The absorbance was linearly dependant on the AC concentrations in the range 0 - 0.05 w/w so that a calibration curve was constructed ( $R^2 = 0.998$ , Fig. 1S, Supplementary material) to subsequently determine AC concentrations in saline suspensions.

#### 2. 5. 2. Optical microscopy and bead diameter measurements

Optical microscopy images were acquired using a microscope Olympus 315 CX41RF (Tokyo, Japan). Bead diameters were determined by using photographs of the beads placed in a Petri dish over a millimeter grid and a camera HDR-CX210 (Sony, Japan). The average bead diameter was calculated from measurements of at least 20 beads using the image analysis program —CellA316 (Olympus, Tokyo, Japan).

#### 2. 5. 3. Surface area analyses

Surface area analysis was performed on ZnA and ZnA/AC beads as well as on AC powder. Samples were degassed at 105 °C for 10 h under reduced pressure and nitrogen adsorption–desorption experiments were performed at a constant temperature by using an ASAP 2020 instrument (Micromeritics, USA). The specific surface area ( $S_p$ ) of samples was calculated according to the Brunauer, Emmett, Teller (BET) method from the linear part of the nitrogen adsorption isotherm [31]. The total pore volume ( $V_{tot}$ ) was calculated from the uptake at  $p/p^0 = 0.998$ . The volume of mesopores ( $V_{meso}$ ) and pore size distribution were analysed according to the Barrett, Joyner and Halenda method from the desorption isotherm [32]. The volume of micropores ( $V_{micro}$ ) was calculated according to t-plot analysis [33] using the Harkins – Jura thickness curve.

#### 2. 5. 4. Field - emission scanning electron microscopy [FE-SEM]

Randomly selected dry cross-sectioned ZnA and ZnA/AC beads were cross-sectioned by using a scalpel. The obtained cross-sections and AC powder were gold coated and examined by MIRA 3 XMU Field Emission Scanning Electron Microscope (Tescan USA Inc., Cranberry Twp, PA).

#### 2. 5. 5. Flame atomic absorption spectrometry [FAAS]

A Perkin Elmer 3100 spectrometer (Perkin Elmer, Analyst 300, USA) was used to determine  $Zn^{2+}$  concentrations in saline and gelling solutions, as well as total  $Zn^{2+}$  contents in the beads (ZnA and ZnA/AC). For determination of the total  $Zn^{2+}$  content, dry beads (0.1g) were dissolved overnight in 9.9 ml aqueous solution of Na – citrate (2 % w/w), centrifuged at 5000 g for 5 min in order to remove AC particles and then, proper dilutions were measured by FAAS.

#### 2. 5. 6. FT-IR analyses

Fourier-transform infrared [FTIR] spectra of ZnA and ZnA/AC beads, as well as AC powder, were recorded in the transmission mode between 4000 - 400  $cm^{-1}$  using a BOMEM (Hartmann & Braun, Frankfurt, Germany) spectrometer with a resolution of 4  $cm^{-1}$  at room temperature. The samples were pressed into pellets with potassium bromide (KBr) and scanned.

### 3. RESULTS

#### 3. 1. Characterization of composite beads

Composite ZnA/AC beads were successfully obtained by extrusion of the suspension (20 % w/w AC and 0.5 % w/w alginate) into a gelling bath that contained  $Zn^{2+}$ . The beads were approximately spherical ( $3.9 \pm 0.1$  mm in diameter), and the spherical shape was practically retained upon drying (diameter of  $3.4 \pm 0.1$  mm) (Fig. 1). The spherical form was chosen in this work as suitable to straightforwardly determine AC release kinetics while different hydrogel shapes can be also produced such as fibres, sheets and films (Fig. 2S, Supplementary material) by well-known techniques.

Textural parameters of dry ZnA/AC beads and AC powder are shown in Table 1. The specific surface area [ $S_p$ ] of ZnA beads was too low and could not be determined. As expected, the AC powder showed somewhat higher  $S_p$  than ZnA/AC composite beads. Slight decreases in  $S_p$  (approximately 10 %) and total pore volume in ZnA/AC beads as compared to those in AC powder could be related to alginate polymer deposition within AC pores as suggested in literature [34]. Average pore diameters were not significantly different indicating in overall that the porosity of AC within the beads was retained.

Table 1. Textural parameters of ZnA/AC beads and AC powder

	$S_p / m^2 g^{-1}$	$V_{tot} / cm^3 g^{-1}$	$V_{meso} / cm^3 g^{-1}$	$V_{micro} / cm^3 g^{-1}$	$D / nm$
ZnA/AC	1009.60	0.5687	0.2446	0.4738	2.94
AC (powder)	1109.05	0.6303	0.2779	0.5194	3.01

$S_p$  – specific surface area;  $V_{tot}$  – total pore volume;  $V_{meso}$  – volume of mesopores;  $V_{micro}$  – volume of micropores;  $D$  – average pore diameter.

FT-IR spectra and FE-SEM micrographs of ZnA and ZnA/AC beads as well as of AC powder are shown in Figure 2.

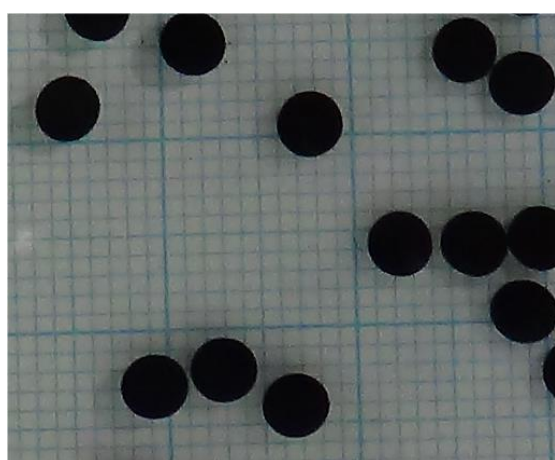


Figure 1. Dry ZnA/AC beads

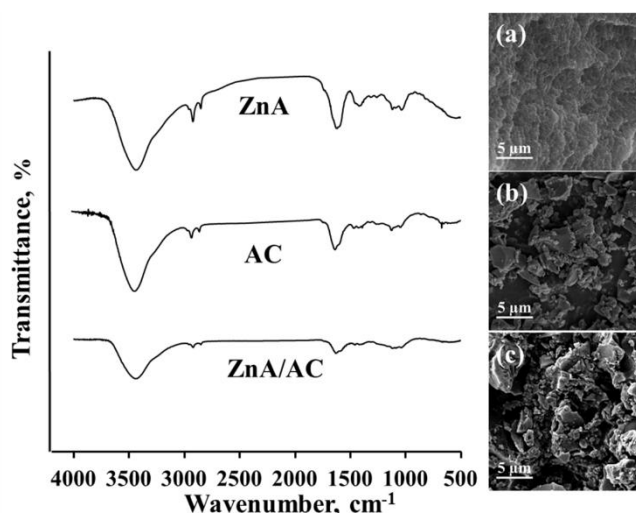


Figure 2. FT-IR spectra of ZnA beads, AC and ZnA/AC beads, and FE-SEM micrographs (insets): (a) cross-section of dry ZnA beads; (b) AC powder; (c) cross-section of dry ZnA/AC beads (scale bar = 5  $\mu m$ )

In both AC and alginate spectra, there is a broad band at  $3440\text{ cm}^{-1}$  which corresponds to O-H stretching vibrations in carboxylic groups, but also in OH groups of alginate or phenolic groups in AC. Both samples also show a double band at  $2925\text{ cm}^{-1}$  and  $2850\text{ cm}^{-1}$  originating from asymmetric and symmetric behaviour of  $\text{CH}_2$  group. The weak band at  $1740\text{ cm}^{-1}$  in AC corresponds to carbonyl groups (in ketone, aldehyde, carboxylic group or its anhydride). Bands at  $1630\text{ cm}^{-1}$  and  $1600\text{ cm}^{-1}$  are related to C=O and C=C aromatic ring vibrations. In the alginate spectrum, the band at  $1628\text{ cm}^{-1}$  rises only from the asymmetric stretching vibrations of the carboxylate groups of mannuronate and guluronate units, while stretching vibrations of the carboxylic acid are seen as a weak shoulder at  $1743\text{ cm}^{-1}$  (asymmetric) and as bands near  $1400\text{ cm}^{-1}$  (symmetric stretching). The aromatic C=C bondage is seen in the AC spectrum as a relatively weak, but well-developed band at  $1465\text{ cm}^{-1}$ . The AC spectrum also indicates that S=O groups are not present since strong bands are not visible in the regions between  $1372\text{--}1335$  and  $1195\text{--}1150\text{ cm}^{-1}$ . Both AC and alginate show non-characteristic bands in the fingerprint region ( $\sim 1200\text{ cm}^{-1} - 800\text{ cm}^{-1}$ ) that correspond mostly to C-O vibrations. However, the most pronounced band in the AC spectrum in this region is at  $1120\text{ cm}^{-1}$  while in the alginate spectrum it is at  $1030\text{ cm}^{-1}$ . The spectrum of ZnA/AC mostly resembles that of AC, which is present at much higher concentration than alginate in the beads. Although chemically very different, the spectra of AC and alginate have the strongest absorption bands similarly positioned, so that the presence of alginate is seen only in the fingerprint region, with the band at  $1030\text{ cm}^{-1}$  being more pronounced in the composite beads than in AC. The intensities of this band and the band at  $1120\text{ cm}^{-1}$  are almost the same in these beads, while their intensity ratios differ in both AC and alginate, as aforementioned.

Morphology of ZnA and ZnA/AC beads, as well as of AC powder, was analysed by FE-SEM (Fig. 2, insets). Cross-sections of ZnA/AC beads showed rough morphology with visible AC particles (Fig. 2c inset) that appeared similar to the initial AC particles (Fig. 2b inset). On the contrary, the cross-section of ZnA beads showed uniform continuous hydrogel matrix as expected (Fig. 2a inset).

### 3. 2. AC release kinetics

Release rates of AC particles were studied in the physiological saline solution during the period of 5 days. The beads retained configuration although changed in size over time. In specific, over the first hour in saline, the beads slightly swelled from  $3.4 \pm 0.1\text{ mm}$  to  $3.6 \pm 0.1\text{ mm}$  in diameter but after 5 h, the bead diameter started to decrease due to AC release so that after 5 days it amounted to  $\sim 2.6\text{ mm}$ . Still the beads were apparently intact without visible fractures although rough surfaces could be noticed (Fig. 3).

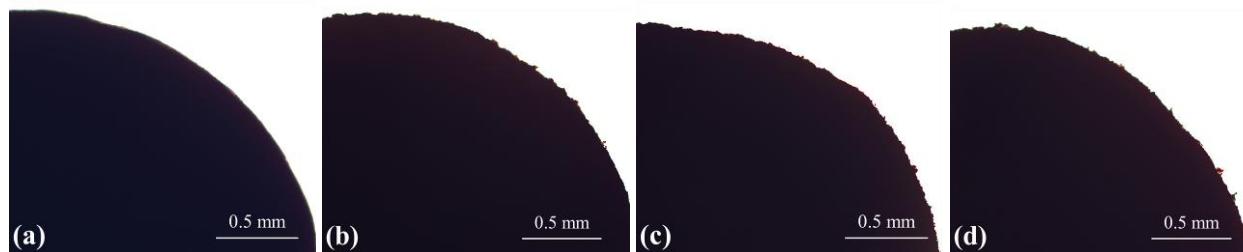


Figure 3. Optical micrographs of the surface of ZnA/AC beads immersed in saline solution at: (a) the initial time point; (b) after 24 h; (c) after 48 h; (d) after 5 days; (scale bar = 0.5 mm)

Measurements of released AC amounts by UV-Vis spectroscopy revealed that the ZnA/AC beads released around 60 % of the initial AC content over the 5-day period (Fig. 4).

Since the beads retained the spherical shape without visible erosion, the experimental data were modelled by diffusion model, which for a spherical particle for short times ( $M_t/M_\infty < 0.4$ ) takes the form [35]:

$$\frac{M_t}{M_\infty} = 6\sqrt{\frac{Dt}{\pi R^2}} - \frac{3Dt}{R^2} \quad (1)$$

where  $M_t$  and  $M_\infty$  denote the cumulative amounts of the substance released at time  $t$  and at infinite time, respectively,  $D$  is the diffusion coefficient of the substance within the sphere, and  $R$  represents the radius of the sphere. The second term in the right-hand side of the Eq. (1) usually can be neglected so that the diffusion coefficient can be determined from the slope of the plot  $M_t/M_\infty$  vs.  $t^{0.5}$ .

Although the average bead diameter in the saline solution slightly varied over time, diffusion model could be successfully applied to the experimental data ( $R^2 > 0.9$ ) (Fig. 4 inset). In specific, over the initial release period of 24 h ( $M_t/M_\infty < 0.4$ , Fig. 4), the bead diameter was in the range from 3 - 3.6 mm, yielding the apparent diffusion coefficient  $D$  of  $\sim 3 \times 10^{-13}\text{ m}^2\text{ s}^{-1}$  for AC in Zn-alginate composite beads immersed in saline solution.

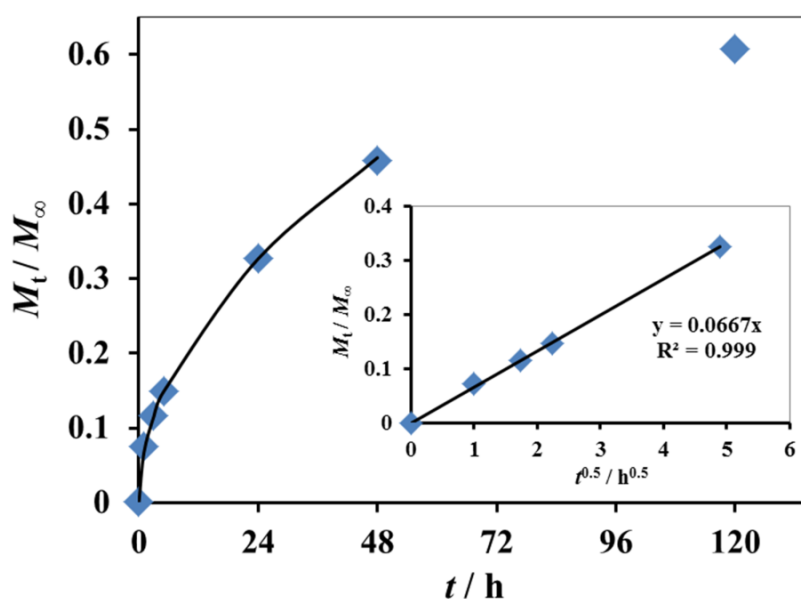


Figure 4. Cumulative release of AC particles from ZnA/AC beads ( $M_t$ ) normalized per the initial AC content ( $M_\infty$ ) over 5 days in the physiological saline solution: experimental data [symbols] and predictions of the diffusion model in the initial release period (line); inset: application of the diffusion model in the initial release period versus  $t^{0.5}$ ; (experimental values are mean  $\pm$  standard deviation ( $SD < 2\%$ ) of  $n=3$ ).

### 3. 3. $Zn^{2+}$ release

Total  $Zn^{2+}$  contents (expressed as  $\mu\text{mol}$  of  $Zn^{2+}$  per g of alginate hydrogel wet weight) in ZnA and ZnA/AC beads were determined by FAAS yielding not statistically different values of  $64.3 \pm 2.9$  and  $63.6 \pm 1.7 \mu\text{mol/g}$ , respectively. Corresponding to the same total  $Zn^{2+}$  contents, release rates of  $Zn^{2+}$  in the physiological saline solution at  $37^\circ\text{C}$  during the 5-day period were also similar for ZnA and ZnA/AC beads (Fig. 3S, Supplementary data). In specific, in the first hour, approximately 75 % of the total  $Zn^{2+}$  content was released in both cases and the  $Zn^{2+}$  concentration in the solution stayed constant over 5 days at  $321.9 \pm 10.3$  and  $310.3 \pm 3.1 \text{ mg dm}^{-3}$ , for ZnA and ZnA/AC beads, respectively. These results indicate that  $Zn^{2+}$  was rapidly exchanged with  $Na^+$  from the saline solution reaching the equilibrium within 1 hour. Since the saline solution was not changed during the 5-day period, the beads did not further release  $Zn^{2+}$  and, although significantly swollen, retained the spherical shape (Fig. 3 and Fig. 4S, Supplementary material).

### 3. 4. Antibacterial activity

Antibacterial activity of ZnA/AC beads was investigated in suspensions of one representative Gram negative bacteria *E. coli* ATCC 25922 (Fig. 5) while ZnA beads and AC powder were used as controls.

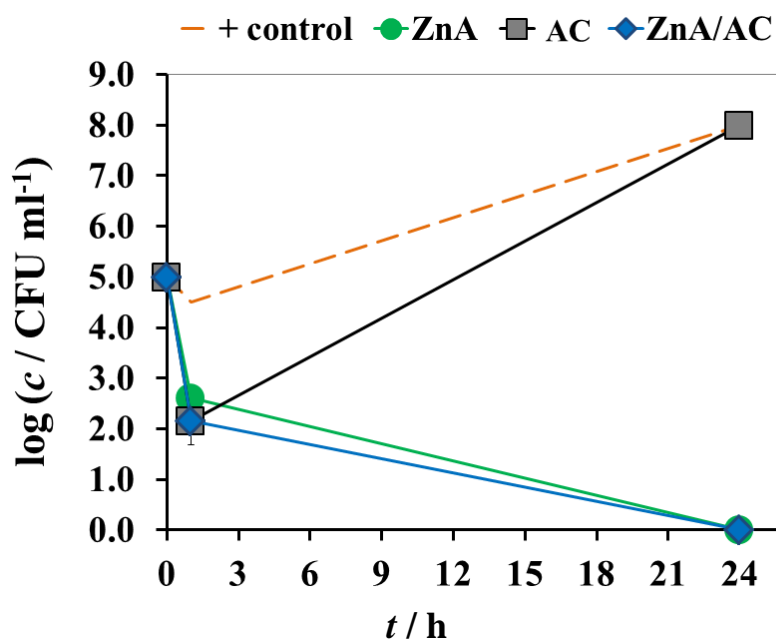


Figure 5. Antibacterial activity of ZnA/AC beads against *E. coli* ATCC 25922; controls were bacterial suspension (+ control), AC particles and ZnA beads; results are expressed as  $\log(c / \text{CFU ml}^{-1})$  and are average of  $n = 2$ .

Results show that ZnA and ZnA/AC composite beads, as well as AC powder alone, induced negative effect on the growth of *E. coli* after 1 hour of contact – time only. The number of viable bacteria in all three suspensions were 2 – 2.5 order of magnitude lower as compared to the positive control. However, in the case of AC powder, this effect was only temporary since after 24 h the microbial count was statistically the same as in the positive control of the bacterial suspension alone. On the contrary, after 24 h, ZnA and ZnA/AC beads induced bactericidal effects by releasing  $Zn^{2+}$  into the broth (Fig. 5). It could be assumed that in this case almost all  $Zn^{2+}$  was released into the broth since ZnA beads formed gelatinous fragments while ZnA/AC beads decreased in size.

#### 4. DISCUSSION

In this study, a system based on Zn-alginate hydrogel with controlled delivery of AC particles and  $Zn^{2+}$  ions were developed in the form of composite ZnA/AC beads. It should be added, that the composite ZnA/AC hydrogel could be produced in other forms such as fibres, films and sheets. The system is intended for wound treatments in which the hydrogel will absorb the wound exudate while the efficient and simultaneous release of two active agents will provide adsorption of toxins, malodour molecules and degradation products by AC particles, as well as antimicrobial effects and enhancement of wound healing by zinc ions.

In our earlier studies, we have optimized the composition of AC suspension in Na-alginate solution (20 % w/w of AC and 0.5 % w/w of Na-alginate) so to produce composite calcium alginate/AC beads with the most efficient AC release [36]. In the present study, we have used this formulation for production of composite zinc alginate/AC beads. The obtained ZnA/AC beads were spherical while the structural analysis revealed rough surface and visible AC particles at bead cross sections similar to the initial ones. Although the  $S_p$  and  $V_{tot}$  of the composite beads were slightly decreased as compared to AC powder, the porosity of AC particles inside the beads was retained. In addition, the FT-IR spectrum of the composite beads appeared more similar to that of AC than of alginate.

Composite ZnA/AC beads efficiently released AC particles and  $Zn^{2+}$  upon the contact with physiological saline solution as a model of biological fluids. It should be noted that pH of the saline solution used in this work was about 5.5 while in chronic wounds it is between 7.15 – 8.9 [37]. Still, higher swelling degrees and faster drug release were observed in alkaline environments as compared to acidic conditions [38], so that even slightly higher release rates could be expected in the wound environment as compared to saline solution. In this work, AC particles were released over a 5-day period by diffusion with the apparent diffusion coefficient estimated as  $\sim 3 \times 10^{-13} \text{ m}^2 \text{ s}^{-1}$ . On the contrary,  $Zn^{2+}$  was released rapidly in the first hour from both ZnA and ZnA/AC beads reaching the equilibrium between the bound and released ions. In addition, total zinc contents in ZnA and ZnA/AC beads were not significantly different ( $\sim 64 \mu\text{mol/g}$ ). This value is in accordance with literature data reported for Zn-alginate microbeads with significantly higher alginate concentration (*i.e.* 1.9 % w/w vs. 0.5 % w/w in the present work) in which the total  $Zn^{2+}$  content was determined as  $159 \pm 7 \mu\text{mol/g}$  [39]. The obtained results imply that AC did not interfere with  $Zn^{2+}$ . However, there are opposite findings regarding  $Zn^{2+}$  adsorption onto AC particles in literature with some reports of high affinity [40, 41] and some of very low affinity of AC towards Zn ions [42]. Yet, the high adsorption rates of metal ions reported usually from wastewaters should not be attributed to activated charcoal only but also to very low initial concentrations of these cations contained in wastewaters (*i.e.* in the order of 100 mg/l vs. 3.9 g/l in the present work) [41]. Furthermore, adsorption of metal ions is determined by functional groups present on AC surface, tailored by the preparation method. Zn was reported to bind to functional groups containing sulfur such as S=O functional groups on the AC surface [40]. In our study, we have used AC that was steam activated so the functional groups containing sulfur were absent, which was also confirmed by FT-IR analyses (Fig. 2). Consequently, in our study  $Zn^{2+}$  did not interact with AC surfaces.

Regarding the functionality in potential wound dressings, the obtained composite ZnA/AC, as well as control ZnA beads, were demonstrated to induce bactericidal effects against one standard Gram negative bacteria, *E. coli*. During the first hour, the significant reduction of the bacterial count was obtained by AC particles alone as well, as it was also reported in the literature [28,43] but the effect was only temporary and after 24 h the bacterial count reached that in the positive control. Thus, it could be assumed that the initial bacterial reduction in the suspension was due to adsorption on AC surfaces as it was also reported in literature [28]. However, AC by itself does not affect bacteria so that they continued to multiply and eventually detached the AC surfaces [44]. So, in order to establish a long-term antibacterial effect, the presence of an antibacterial substance was necessary.  $Zn^{2+}$  release studies have shown that this cation was quickly released from both ZnA and ZnA/AC beads reaching the equilibrium concentration in the saline solution of about 5 mM. This  $Zn^{2+}$  concentration is in the range of minimum inhibitory concentrations [MIC] reported for many Gram positive [45] and Gram negative bacteria [45,46]. In the present study, the released  $Zn^{2+}$  concentration in the tryptone soya broth was probably even higher as assumed from the hydrogel appearance so it efficiently eradicated bacteria from the suspension.

## 5. CONCLUSION

In this work, we have produced a multifunctional antibacterial composite based on a zinc-alginate hydrogel and AC particles. Upon contact with physiological-like environment, AC particles and Zn<sup>2+</sup> were simultaneously and efficiently released. By controlled release, AC particles are intended to establish direct contact with the wound fluids and adsorb wound products as well as bacterial cells. However, the reduction of bacterial count in the present study was only short-term imposing the need for an antibacterial agent such as Zn<sup>2+</sup> for inducing bactericidal effects. AC particles did not interact with Zn<sup>2+</sup> so that the released concentration of this cation from composite beads in physiological saline solution was ~5 mM, which was sufficient to eliminate *E. coli* from the suspension. Bearing in mind that zinc ions have been also shown to promote wound healing, the presented approach based on a simple composite consisting of only three components has shown potentials for realizing a versatile and affordable wound dressing.

**Acknowledgement:** *This work was supported by the Ministry of Education, Science and Technological Development of the Republic of Serbia (Grant III 45019). The authors would like to thank Dr. Djordje Veljovic, Faculty of Technology and Metallurgy, University of Belgrade, Serbia, for the assistance in performing FE-SEM analyses.*

## REFERENCES

- [1] Williams K, Griffiths E. Malodorous wounds: causes and treatment. *Nurs Residential Care*. 1999; 1 (5): 276-285.
- [2] Wilson V. Assessment and management of fungating wounds: a review. *Br J Community Nurs*. 2005; 10 (3): S28-34.
- [3] McDonald A, Lesage P. Palliative management of pressure ulcers and malignant wounds in patients with advanced illness. *J Palliat Med*. 2006; 9 (2): 285–295.
- [4] Grocott PA. Review of advances in fungating wound management since EWMA 1991. *EWMA J*. 2002; 2 (1), 21-24.
- [5] Alexander S. Malignant fungating wounds: key symptoms and psychosocial issues. *J Wound Care*. 2009; 18 (8): 325-329.
- [6] Bishop SM, Walker M, Rogers AA, Chen WYJ. Importance of moisture balance at the wound-dressing interface. *J Wound Care* 2003; 12 (4): 125-128.
- [7] Nazarko L. Malignant fungating wounds. *Nurs Residential Care*. 2006; 8 (9): 402-406.
- [8] Landsdown A. Calcium: a potential central regulator in wound healing in the skin. *Wound Repair Regen*. 2002; 10: 271–285.
- [9] Stenvik J, Sletta H, Grimstad O, Pukstad B, Rzan L, Aune R, Strand W, Tondervik A, Torp SH, Skjak-Braek G, Espevik T. Alginates induce differentiation and expression of CXCR7 and CXCL12/SDF-1 in human keratinocytes – the role of calcium. *J Biomed Mater Res A*. 2012; 100: 2803–2812.
- [10] Stojkowska J, Djurdjevic Z, Jancic I, Bufan B, Milenkovic M, Jankovic R, Miskovic-Stankovic V, Obradovic B. Comparative *in vivo* evaluation of novel formulations based on alginate and silver nanoparticles for wound treatments, *J. Biomater. Appl*. 2018; 32 (9): 1197-1211.
- [11] Qin Y. Alginate fibres: an overview of the production processes and applications in wound management, *Polym Int*. 2008; 57: 171–180.
- [12] Haase H, Overbeck S, Rink L. Zinc supplementation for the treatment or prevention of disease: current status and future perspectives, *Exp. Gerontol*. 2008; 43: 394–408.
- [13] Leung YH, Chan CMN, Ng AMC, Chan HT, Chiang MWL, Djuricic AB, Ng YH, Jim WY, Guo MY, Leung FCC, Chan WK, Au DTW. Antibacterial activity of ZnO nanoparticles with a modified surface under ambient illumination, *Nanotechnology*. 2012; 23 (47): 475703.
- [14] Vallee B L, Falchuk H. The biochemical basis of zinc physiology, *Physiol. Rev*. 1993; 73: 79-118.
- [15] Eide D. Zinc transporters and the cellular trafficking of zinc. *Biochimica et Biophysica Acta (BBA) - Molecular Cell Research*. 2006; 1763 (7): 711-722.
- [16] Bafaro E, Liu Y, Xu Y, Dempski RE. The emerging role of zinc transporters in cellular homeostasis and cancer. *Signal Transduct Target Ther*. 2017; 2: 17029.
- [17] Borovansky J, Riley PA. Cytotoxicity of zinc *in vitro*. *Chem. Biol. Interact*. 1989; 69: 279–291.
- [18] Lipovsky A, Nitzan Y, Gedanken A, Lubart R. Antifungal activity of ZnO nanoparticles—the role of ROS mediated cell injury. *Nanotechnology*. 2011; 22: 105101.
- [19] Atmaca S, Gül K, Cicek R. The effect of zinc on microbial growth *Turk. J. Med.Sci*. 1998; 28: 595–597.
- [20] Padmavathy N, Vijayaraghavan R. Enhanced bioactivity of ZnO nanoparticles—an antimicrobial study. *Sci. Technol. Adv. Mater*. 2008; 9: 035004.
- [21] Zhang L, Jiang Y, Ding Y, Daskalakis N, Jeuken L, Povey M, O'Neill AJ, York DW. Mechanistic investigation into antibacterial behaviour of suspensions of ZnO nanoparticles against *E. coli*. *J. Nanopart. Res*. 2010; 12: 1625–1636.
- [22] Miller LP, McCallan SEA. Toxic action of metal ions to fungus spores. *J. Agric.Food Chem*. 1957; 5: 116–122.
- [23] Lansdown ABG, Path FRC, Mirastschijski U, Stubbs N, Scanion E, Agren MS. Zinc in wound healing: theoretical, experimental and clinical aspects. *Wound repair and regeneration*. 2007; 15: 2–16.
- [24] Lin P-H, Sermersheim M, Li H, Lee PHU, Steinberg SM, Ma J, Zinc in wound healing modulation, *Nutrients*, 2017; 10 (1).

- [25] Cole L. The effect of coupled haemofiltration and adsorption on inflammatory cytokines in an *ex vivo* model. *Nephrology Dialysis Transplantation*. 2002; 17 (11): 1950-1956.
- [26] Howell C, Sandeman S, Phillips G, Lloyd A, Davies J, Mikhailovsky S, Tennison S, Rawlinson A, Kozynchenko O, Owen H, Gaylor J, Rouse J, Courtney J. The *in vitro* adsorption of cytokines by polymer-pyrolysed carbon. *Biomaterials*. 2006; 27 (30): 5286-5291.
- [27] Kerihuel J. Effect of activated charcoal dressings on healing outcomes of chronic wounds. *Journal of Wound Care*. 2010; 19 (5): 208-214.
- [28] Naka K, Watarai S, Tana Inoue K, Kodama Y, Oguma K, Yasuda T, Kodama H. Adsorption Effect of Activated Charcoal on Enterohemorrhagic *Escherichia coli*. *Journal of Veterinary Medical Science*. 2001; 63 (3): 281-285.
- [29] Sandeman S, Howell C, Mikhailovsky S, Phillips G, Lloyd A, Davies J, Tennison S, Rawlinson A, Kozynchenko O. Inflammatory cytokine removal by an activated carbon device in a flowing system. *Biomaterials*. 2008; 29 (11): 1638-1644.
- [30] Atkins P, de Paula, Physical Chemistry, 9th Edition, 2010; Oxford: Oxford University Press.
- [31] Rouquerol F, Rouquerol J, Sing K. Adsorption by Powders and Porous Solids. 1975; London: Academic Press.
- [32] Barrett E, Joyner L, Halenda P. The Determination of Pore Volume and Area Distributions in Porous Substances. I. Computations from Nitrogen Isotherms. *Journal of the American Chemical Society*. 1951; 73 (1): 373-380.
- [33] Lippens B. Studies on pore systems in catalysts V. The t method. *Journal of Catalysis*. 1965; 4 (3): 319-323.
- [34] Hassan A, Abdel-Mohsen A, Fouda M. Comparative study of calcium alginate, activated carbon, and their composite beads on methylene blue adsorption. *Carbohydrate Polymers*. 2014; 102: 192-198.
- [35] Siepmann J, Siepmann F. Modeling of diffusion controlled drug delivery. *Journal of Controlled Release*. 2012; 161 (2): 351-362.
- [36] Osmokrovic A, Obradovic B. Polymer composites based on alginate and activated charcoal, patent application RS 20150403 (A1), 2015.
- [37] Gethin G. The significance of surface pH in chronic wounds, *Wounds UK*. 2007; 3:52-56.
- [38] Chuang J-J, Huang Y-Y, Lo S-H, Hsu T-F, Huang W-Y, Huang S-L, Lin Y-S. Effects of pH on the Shape of Alginate Particles and Its Release Behavior, *International Journal of Polymer Science*. 2017; Article ID 3902704, 9 pages. <https://doi.org/10.1155/2017/3902704>.
- [39] Malagurski I, Levic S, Pantic M, Matijasevic D, Mitric M, Pavlovic V, Dimitrijevic-Brankovic S. Synthesis and antimicrobial properties of Zn-mineralized alginate nanocomposites, *Carbohydrate Polymers*. 2017; 165: 313-321.
- [40] Madhava Rao M, Chandra Rao GP, Seshaiiah K, Choudar NV, Wang MC. Activated carbon from *Ceiba pentandra* hulls, an agricultural waste, as an adsorbent in the removal of lead and zinc from aqueous solutions, *Waste Management*. 2008; 28: 849-858.
- [41] Kouakou U, Ello AS, Yapo JA, Trokourey A. Adsorption of iron and zinc on commercial activated carbon. *Journal of Environmental Chemistry and Ecotoxicology*. 2013; 5 (6): 168-171.
- [42] Gyu Parl H, Won Kim T, Yun Chae M, Yoo I-K. Activated carbon-containing alginate adsorbent for the simultaneous removal of heavy metals and toxic organics, *Process Biochemistry*. 2007; 42: 1371-1377.
- [43] Muller G, Winkler Y, Kramer A. Antibacterial activity and endotoxin-binding capacity of Actisorb<sup>®</sup> Silver 220. *Journal of Hospital Infection*, 2003; 53 (3): 211-214.
- [44] Osmokrovic A, Jancic I, Vunduk J, Petrovic P, Milenkovic M, Obradovic B. Achieving high antimicrobial activity: Composite alginate hydrogel beads releasing activated charcoal with an immobilized active agent. *Carbohydrate Polymers*. 2018; 196: 279-288.
- [45] Aarestrup F, Hasman H. Susceptibility of different bacterial species isolated from food animals to copper sulphate, zinc chloride and antimicrobial substances used for disinfection. *Veterinary Microbiology*. 2004; 100: 83-89.
- [46] Brocklehurst K, Morby A P. Metal-ion tolerance in *Escherichia coli*: analysis of transcriptional profiles by gene-array technology. *Microbiology*. 2000; 146: 2277-2282.

**SAŽETAK****Novi kompoziti na bazi cink-alginatnog hidrogela sa sadržanim česticama aktivnog uglja za potencijalnu primenu u primarnim, multifunkcionalnim oblogama za rane**

Andrea Osmokrovića, Ivan Jančić<sup>b</sup>, Ivona Janković-Častvan<sup>a</sup>, Predrag Petrović<sup>c</sup>, Marina Milenković<sup>b</sup>, Bojana Obradović<sup>a</sup>

<sup>a</sup>Tehnološko-metalurški fakultet, Univerzitet u Beogradu, Karnegijeva 4, 11000 Beograd, Srbija

<sup>b</sup>Farmaceutski fakultet, Univerzitet u Beogradu, Vojvode Stepe 450, 11000 Beograd, Srbija

<sup>c</sup>Inovacioni centar TMF, Karnegijeva 4, 11000 Beograd, Srbija

(Naučni rad)

U ovom radu, dobijeni su novi kompoziti u obliku čestica na bazi Zn-alginatnog hidrogela ekstruzijom smeše sastava 0,5 mas. % alginata i 20 mas. % aktivnog uglja [AU] sa ciljem istovremenog otpuštanja dve aktivne supstance iz kompozita u fiziološkim uslovima, i to jone cinka i čestice AU. Dobijene kompozitne čestice su analizirane primenom skenirajuće elektronske mikroskopije i karakterisane u pogledu teksturalnih karakteristika, kao i kinetike otpuštanja jona cinka i čestica AU u fiziološkom rastvoru. Joni cinka su se brzo otpustili u rastvor tako da je postignuta ravnoteža u toku prvog sata otpuštanja, nasuprot otpuštanja čestica AU koje je opisano modelom unutrašnje difuzije sa prividnom difuzivnošću od oko 10-13 m<sup>2</sup> s<sup>-1</sup>. Potencijalna funkcionalnost kompozita je procenjena u pogledu antibakterijske aktivnosti u suspenziji standardnog soja *Escherichia coli* 25922. Uočen jak baktericidan efekat je pripisan brzom otpuštanju jona cinka na koje nije uticalo prisustvo čestica AU. Uzevši u obzir rezultate dobijene u ovom radu, kao i veliki sorpcioni kapacitet alginatnog hidrogela, efikasnost AU da adsorbuje neprijatne mirise i raspadne produkte u rani, i pozitivne efekte jona cinka na zarastanje rana, može se zaključiti da su razvijeni kompoziti pokazali značajan potencijal za primenu kao multifunkcionalne obloge za rane.

*Ključne reči:* joni cinka, aktivni ugalj, alginatni hidrogel, antibakterijska aktivnost, obloge za rane